

# Noncommutative Inspired Black Holes in Extra Dimensions <sup>\*</sup> <sup>†</sup>

Thomas G. Rizzo<sup>a</sup>

*Stanford Linear Accelerator Center, 2575 Sand Hill Rd., Menlo Park, CA, 94025*

## Abstract

In a recent string theory motivated paper, Nicolini, Smailagic and Spallucci (NSS) presented an interesting model for a noncommutative inspired, Schwarzschild-like black hole solution in 4-dimensions. The essential effect of having noncommutative co-ordinates in this approach is to smear out matter distributions on a scale associated with the turn-on of noncommutativity which was taken to be near the 4-d Planck mass. In particular, NSS assumed that this smearing was essentially Gaussian. This energy scale is sufficiently large that in 4-d such effects may remain invisible indefinitely. Extra dimensional models which attempt to address the gauge hierarchy problem, however, allow for the possibility that the effective fundamental scale may not be far from  $\sim 1$  TeV, an energy regime that will soon be probed by experiments at both the LHC and ILC. In this paper we generalize the NSS model to the case where flat, toroidally compactified extra dimensions are accessible at the TeV-scale and examine the resulting modifications in black hole properties due to the existence of noncommutativity. We show that while many of the noncommutativity-induced black hole features found in 4-d by NSS persist, in some cases there can be significant modifications due the presence of extra dimensions. We also demonstrate that the essential features of this approach are not particularly sensitive to the Gaussian nature of the smearing assumed by NSS.

---

<sup>\*</sup>Work supported in part by the Department of Energy, Contract DE-AC02-76SF00515

<sup>†</sup>e-mail: <sup>a</sup>rizzo@slac.stanford.edu

# 1 Introduction and Background

The theoretical effort that has gone into understanding the full details of string/M theory has inspired a number of ideas which, on their own, have had a significant impact on particle physics model building and phenomenology. One of the more recent developments of this kind has been the resurgence[1] of interest in noncommutative (NC) quantum field theories[2] and, in particular, the question of how a NC version of the Standard Model (SM) may be constructed[3] and probed experimentally[4].

The essential idea behind NC constructions is that the commutator of two spacetime coordinates, now thought of as operators, is no longer zero. In its simplest form, for a space with an arbitrary number of dimensions,  $D$ , this can be written explicitly as

$$[x_A, x_B] = i\theta_{AB} = i\frac{c_{AB}}{\Lambda_{NC}^2}, \quad (1)$$

where  $\Lambda_{NC}$  is the mass scale associated with NC and  $c_{AB}$  is a *frame-independent*, dimensionless anti-symmetric matrix with constant, real, typically  $O(1)$  entries; it is *not* a tensor. Here we assume that vastly different NC scales do not exist depending upon the values of  $A, B$ . <sup>‡</sup> In a general string theory context one might imagine that  $\Lambda_{NC}$  would naturally not be far from the 4-d Planck scale,  $\overline{M}_{Pl}$ , and that the  $c_{AB}$  are generated due to the presence of background ‘electric’ or ‘magnetic’ type fields. Most of the phenomenological studies of NC models[4] have assumed that we live in 4-d and that  $\Lambda_{NC} \sim 1\text{-}10$  TeV so that we have access to this scale at, *e.g.*, the LHC or ILC. However, if the NC scale  $\Lambda_{NC}$  is indeed of order  $\overline{M}_{Pl}$ , then probing NC physics directly may prove difficult in the near term.

One way of possibly observing NC is its effects on the properties of black holes (BH). In order to analyze this problem at a truly fundamental level one would need to successfully construct the NC equivalent of General Relativity. Attempts along these lines have been made

---

<sup>‡</sup>In what follows, upper case Roman letters will label all  $D$  dimensions while Greek (lower case Roman) letters will cover the range 0-3 (5 to  $n + 4$ ).

in the literature[5] but no complete and fully compelling theory of this type yet exists. Recently, Nicolini, Smailagic and Spallucci (NSS) [6] have considered a physically motivated and tractable model of the possible NC modifications to Schwarzschild BH solutions. The essential ideas of this picture are: (i) General Relativity in its usual commutative form as described by the Einstein-Hilbert action remains applicable. This seems justifiable, at least to a good approximation, if NC effects can be treated perturbatively. The authors in Ref.[5] have indeed shown that the leading NC corrections to the form of the Einstein-Hilbert action are at least second order in the  $\theta_{AB}$  parameters. (ii) NC leads to a ‘smearing’ of matter distributions on length scales of order  $\sim \Lambda_{NC}^{-1}$ . Thus the usual ‘ $\delta$ -function’ matter source of the conventional Schwarzschild solution is replaced by a centrally peaked, spherically symmetric (and time-independent) mass distribution which has a size of order  $\sim \Lambda_{NC}^{-1}$ . This, too, seems justifiable based on the results presented in Ref.[5], which note that matter actions from which the stress-energy tensors are derived are modified at leading order in the  $\theta_{AB}$  parameters. For simplicity, NSS assumed that this smeared distribution takes the form of a spherical 3-d Gaussian in 4-d whose size, due to the spherical symmetry, was set by a single parameter,  $\theta$ , indicative of the NC scale. Though such a picture leads to many interesting properties for the resulting BH (to be elaborated on below), since  $\overline{M}_{Pl} \sim \Lambda_{NC}$  was assumed, as would be natural in 4-d, such BH are not immediately accessible to experiment or to direct observation.

Another interesting prediction of string theory is that several extra dimensions must exist. However, extra spatial dimensions, in models with an effective fundamental scale  $M_*$  now in the TeV range, have been discussed as possible solutions to the hierarchy problem[7, 8]. In the case of ‘flat’ extra dimensions, *e.g.*, in the model of Arkani-Hamed, Dimopoulos and Dvali (ADD)[7], the 4-d Planck and fundamental scales are related by the volume of the compactified extra dimensions:

$$\overline{M}_{Pl}^2 = V_n M_*^{n+2}, \quad (2)$$

where  $V_n$  is the volume of the compactified manifold. Assuming for simplicity that these extra

dimensions form an  $n$ -dimensional torus, if all compactification radii ( $R_c$ ) are the same, then  $V_n = (2\pi R_c)^n$ . In such a scenario gravity becomes strong at  $M_*$  and not at  $\overline{M}_{Pl}$  which is viewed as an artifact of our inability to probe gravity at scales smaller than  $R_c$ . This scenario has gotten a lot of attention over the last few years and the collider phenomenology of these types of models has been shown to be particularly rich[9]. In such a scheme it would be natural that the NC scale,  $\Lambda_{NC}$ , would now also be of order  $M_* \sim \text{TeV}$  allowing it to be accessible to colliders. Furthermore, the copious production of TeV-scale BH at colliders also becomes possible[10] and the nature of such BH could then be examined experimentally in some detail. Thus it is reasonable to ask if the properties of such TeV-scale BH may be influenced by NC effects, which originate at a similar scale, and if these effects are large enough to be observable in collider data.

The goal of the present paper is to begin to address these issues. In particular we will examine how NC BH in  $D$  dimensions differ from those in 4-d as well as from the more conventional  $D$ -dimensional commutative Schwarzschild BH traditionally analyzed at colliders. Furthermore, we will demonstrate that the essential features of this scenario are not particularly sensitive to the detailed nature of the assumed NC smearing.

## 2 Analysis and Results

We begin our analysis by reminding the reader that we will assume that  $D = 4 + n$ -dimensional gravity, and BH in particular, can still be described by the conventional Einstein-Hilbert (EH) action, *i.e.*,

$$S = \frac{M_*^{n+2}}{2} \int d^{4+n}x \sqrt{-g} R, \quad (3)$$

with  $R$  being the Ricci scalar and  $M_*$  being the (reduced) fundamental scale as appearing in the ADD relationship above. It is important to recall that for the ADD scenario with  $n \geq 2$ ,  $M_*$  is only weakly constrained by current collider experiments, *i.e.*, one finds that  $M_* \geq 0.38 - 0.60$  TeV, depending on the value of  $n$ , when the bound on the more commonly used GRW[9] parameter

$M_D > 1.5$  TeV is employed.

In the present and NSS approaches the basic effect of NC is proposed to be the smearing out of conventional mass distributions. Thus, following NSS[6], we will assume, instead of the point mass,  $M$ , described by a  $\delta$ -function distribution, that we have a static, spherically symmetric, Gaussian-smeared matter source whose NC ‘size’ is determined by the parameter  $\sqrt{\theta} \sim \Lambda_{NC}^{-1}$ :

$$\rho = \frac{M}{(4\pi\theta)^{(n+3)/2}} e^{-r^2/4\theta}. \quad (4)$$

Here will we explicitly assume that both the horizon size of our BH and the NC parameter  $\sqrt{\theta}$  are far smaller than the compactification scale  $R_c$  so that the BH physics is not sensitive to the finite size of the compactified dimensions. For ADD-type models this can be easily verified from the numerical results we obtain below as the BH horizon size will typically be of order  $\sim 1/M_*$  while  $R_c$  is generally many orders of magnitude larger as long as the value of  $D$  is not too large[11] and is certainly the case when  $D \leq 11$ . Note that the value of  $\sqrt{\theta}$  is directly correlated with the NC scale and is certainly proportional to it; however, within this treatment the exact nature of this relationship is unspecified and would require a more detailed model to explicitly determine. It is sufficient to remember only that  $\theta \approx 1/\Lambda_{NC}$ . It is important to realize that many such parameterizations of this peaked smeared mass distribution are possible which should lead to qualitatively similar physics results. However, the various predictions arising from these may differ only at the  $O(1)$  level or less, as long as the detailed structure of the peaked mass distribution is not probed. We will discuss this issue further below.

The metric of our  $D$ -dimensional space is assumed to be given by the usual  $D$ -dimensional Schwarzschild form

$$ds^2 = e^\nu dx_0^2 - e^\mu dr^2 - r^2 d\Omega_{D-2}^2. \quad (5)$$

Here we will be searching for Schwarzschild-like, spherically symmetric and static solutions with  $\nu$  and  $\mu$  being functions only of the co-ordinate  $r$  and we will further demand that  $e^{\nu,\mu} \rightarrow 1$  as

$r \rightarrow \infty$ ; this will require that  $\nu = -\mu$  in the solutions of Einstein's equations as in the usual commutative scenario since the EH action and resulting field equations remains applicable. Note that the surface of the sphere,  $\Omega_{D-2}$ , can be simply described by a set of  $D-2 = n+2$  angles,  $\phi_i$ , where  $i = 1, \dots, n+2$ .

Given the assumed form of the matter density,  $\rho$ , above and the expectation that  $\nu = -\mu$  as usual, two components of the diagonal stress-energy tensor,  $T^{AB}$ , are already determined, *i.e.*,  $T_r^r = T_0^0 = \rho$ . As noted by NSS, the remaining components,  $T_i^i$  (no summation), all  $n+2$  of which are identical due to the spherical symmetry, can be obtained from the requirement that  $T^{AB}$  have a vanishing divergence,  $T^{AB};_B = 0$ , where the semicolon denotes covariant differentiation. Given the nature of our assumed metric it is easily seen that both  $T^{00};_0 = 0$  and  $T^{ii};_i = 0$ , for all  $i$ , automatically. The remaining equation  $T^{rr};_r = 0$  then yields the explicit result

$$0 = \partial_r T_r^r + \frac{1}{2} g^{00} (T_r^r - T_0^0) \partial_r g_{00} + \frac{1}{2} \sum_i g^{ii} (T_r^r - T_i^i) \partial_r g_{ii}. \quad (6)$$

Since by construction  $T_r^r = T_0^0$  and, noting that  $g^{ii} \partial_r g_{ii} = 2/r$ , for all (unsummed)  $i$ , this yields

$$T_i^i = \rho + \frac{r}{n+2} \partial_r \rho, \quad (7)$$

for all  $i$  (without summation). This reproduces the 4-d NSS result in the limit when  $n \rightarrow 0$ .

With our assumed metric the non-zero components of the Ricci tensor are given by (with the index  $i$  not summed)

$$\begin{aligned} R_0^0 = R_r^r &= -\frac{e^\nu}{2} \left[ \nu'' + (\nu')^2 + (n+2) \frac{\nu'}{r} \right] \\ R_i^i &= \frac{-1}{r^2} \left[ e^\nu (1 + n + r\nu') - (n+1) \right], \end{aligned} \quad (8)$$

where now a prime denotes partial differentiation with respect to  $r$ . The Einstein equations resulting from the EH action augmented with our matter distribution can be conveniently written in the form

$$R_A^B = \frac{1}{M_*^{n+2}} \left( T_A^B - \delta_A^B \frac{T}{n+2} \right), \quad (9)$$

where  $T$  is the trace of the stress-energy tensor,  $T = T_A^A$ . Note that given our assumptions there are only two distinct Einstein equations. Writing  $g_{00} = e^\nu = 1 - A(r)$ , the  $R_i^i$  Einstein equation leads to the following first order differential equation for  $A(r)$ :

$$A' + \frac{n+1}{r} A = \frac{1}{M_*^{n+2}} \frac{2r\rho}{n+2}, \quad (10)$$

from which we obtain the following solution, after substituting the above expression for  $\rho$  and demanding that  $A(r) \rightarrow 0$  as  $r \rightarrow \infty$ :

$$A(r) = \frac{1}{M_*^{n+2}} \frac{M}{(n+2)\pi^{(n+3)/2}} \frac{1}{r^{n+1}} \int_0^{r^2/4\theta} dt e^{-t} t^{(n+1)/2}. \quad (11)$$

This result is seen to reduce to that of NSS when  $n \rightarrow 0$  as well as to the usual  $D$ -dimensional Schwarzschild solution when  $\theta \rightarrow 0$ . The remaining  $R_0^0$  Einstein equation just gives us back the continuity equation for the stress-energy tensor, hence, nothing new. Note that given our assumptions these results allow us to calculate  $A(r)$  for any assumed form of the mass distribution  $\rho(r)$ .

The horizon radius,  $R_H$ , occurs at values of  $r$  where  $g_{00} = 0$ , *i.e.*, where  $A(r) = 1$ . Defining for convenience the dimensionless quantities  $m = M/M_*$ ,  $x = M_*R_H$  and  $y = M_*\sqrt{\theta}$ , along with the constant

$$c_n = \frac{(n+2)\pi^{(n+3)/2}}{\Gamma(\frac{n+3}{2})}, \quad (12)$$

the horizon radius can be obtained by solving the equation

$$x^{n+1} = \frac{m}{c_n} F_n(z), \quad (13)$$

where  $z = x/y$  and the functions  $F_n(z)$  are given by the integrals

$$F_n(z) = \frac{1}{\Gamma(\frac{n+3}{2})} \int_0^{z^2/4} dt e^{-t} t^{(n+1)/2}. \quad (14)$$

These integrals be performed analytically when  $n$  is odd, *e.g.*,  $F_1 = 1 - e^{-q}(1+q)$ ,  $F_3 = 1 - e^{-q}(1 + q + q^2/2)$  and  $F_5 = 1 - e^{-q}(1 + q + q^2/2 + q^3/6)$ , *etc*, with  $q = z^2/4$ . (For  $n$  even these functions can be expressed in terms of combinations of error functions.) Given their definition it is clear that the  $F_n$  vanish as  $\sim z^{n+3}$  when  $z \rightarrow 0$  and they are seen to monotonically increase with increasing  $z$ ; as  $z \rightarrow \infty$  our normalization is such that  $F_n \rightarrow 1$ . This implies that the BH mass,  $m$ , diverges as either  $x \rightarrow 0, \infty$  for fixed  $y$  and that a minimum value of  $m$  must exist for some value of  $x$ . Since  $x$  appears on both sides of the above equation determining the horizon radius, a trivial relationship between  $m$  and  $x$  no longer occurs as it does for the ordinary  $D$ -dimensional Schwarzschild BH solution. In the  $\theta, y \rightarrow 0$  limit, corresponding to the usual commutative result, the upper limit of the integral defining the functions  $F_n$  becomes infinite and we arrive at the well-known standard result[10] as then  $F_n \rightarrow 1$ :

$$m = c_n x^{n+1}. \quad (15)$$

Note that if we had chosen a different form for the matter distribution representing the smeared point mass source only the set of functions  $F_n(z)$  would be changed but their general properties would be identical to those above. For example, if we had assumed a smearing of the modified Lorentzian form,  $\rho \sim (r^2 + \theta'^2)^{-(n+4)/2}$ , (with the parameter  $\theta'$  not necessarily being the same as  $\theta$ ) then the corresponding functions, which we'll call  $G_n$ , would also vanish as  $z \rightarrow 0$  in a power law manner and go  $\rightarrow 1$  as  $z \rightarrow \infty$  in a monotonic fashion. For example, one obtains  $G_0(z) = \frac{2}{\pi} (\tan^{-1} z - \frac{z}{1+z^2})$  which we observe has these same limiting properties and is quite similar to the  $F_n$  qualitatively. More generally we find that the  $G_n$  are given by the integrals

$$G_n(z) = \frac{2}{\pi} \frac{(n+2)!!}{(n+1)!!} \int_0^z dt \frac{t^{n+2}}{(1+t^2)^{(n/2+2)}}. \quad (16)$$

These basic properties of the  $F_n$  (and  $G_n$ ) capture the essential aspects of the NC physics. Other possible smearings, such as a straightforward exponential, would also lead to quite similar results.<sup>§</sup> We will have more to say about this below but note that many of the specific expressions that we will obtain remain applicable if we assume a different form for the smeared mass distribution.

It is interesting to inquire how the NC value of  $x$ , for the moment explicitly denoted as  $x_{NC}$ , compares with the usual  $D$ -dimensional result. Clearly for any fixed value of  $m$  the ratio  $x_{NC}/x$  can be expressed solely via the functions  $F_n$  and is thus only dependent upon the ratio  $z = x/y$  and  $n$ ; the result of this calculation is shown in Fig. 1. In examining these results, as well as those in the following figures, it is important to remember that when  $n = 0$ ,  $M_* = \overline{M}_{Pl}$ ; for all larger values of  $n$ ,  $M_* \sim 1$  TeV. In this figure we see that for large values of  $z \gtrsim 3$  we recover the commutative result for all  $n$  since the NC scale is far smaller than the horizon size in this case. However when the two scales are comparable or when the horizon shrinks inside the NC scale the value of  $x$  is greatly reduced for fixed  $m$ . Of course, we really should not trust the details of our modeling of the NC effects when  $z$  is extremely small, *i.e.*, when  $x$  is very much less than  $y$ . It is also in this very region where most of the differences between, *e.g.*, the Gaussian and Lorentzian forms of the smeared mass distribution would be expected to begin to appear.

More generally, we can now calculate  $m$  as a function of  $x$  for fixed  $y$ . Instead of a monotonically increasing function  $\sim x^{n+1}$ , we find that  $m(x)$  is now a function with a single minimum and which grows large as either  $x \rightarrow 0$  or  $\rightarrow \infty$ . For small  $x$  we find the scaling  $m \sim y^{n+3}/x^2$  while the usual commutative behavior is obtained at large  $x$ ,  $\sim x^{n+1}$ . Fig. 2 gives a first rough indication of this behavior. The existence of a minima has several implications: (*i*) a minimum value of  $m$  implies that there is a physical mass threshold below which BH will not form. (*ii*) The inverse function,  $x(m)$ , is double valued indicating the existence of two possible horizons for a fixed value of the BH mass; this is a potentiality first pointed out by NSS and something we will return

---

<sup>§</sup>For the case of an exponential, the corresponding functions,  $Q_n(z)$ , are found to be related to the  $F_n$  above as  $Q_n(z) = F_{2n+3}(z^2/4)$ .

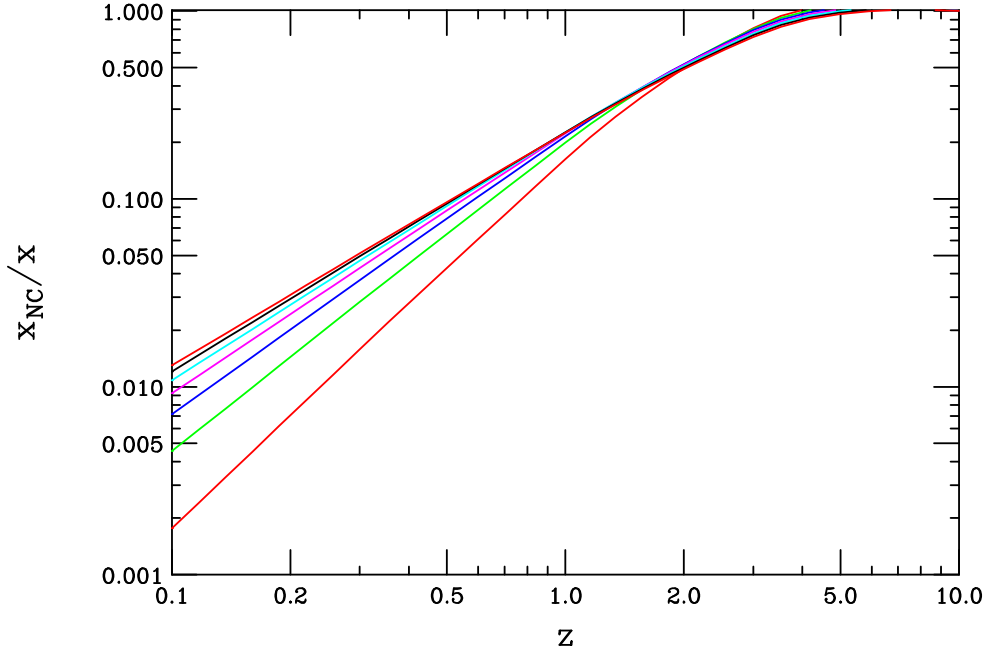


Figure 1: Horizon size in the NC scenario compared to the commutative result as a function of  $z = x/y$  for fixed values of  $m$ . On the left-hand side of the figure, from bottom to top, the curves correspond to  $n = 1$  to  $7$ .

to below. In Fig. 2 we see several additional features: first, as  $y$  increases for fixed  $n$  so does  $m$  except where  $x$  is large and we are thus residing in the commutative limit. Also for large  $y$  we see that  $m$  increases with  $n$  as it usually does in the commuting case. This is not too surprising given the small  $x$  scaling behavior of  $m$  above. Secondly, we see that for large  $y$  the values  $m$  are always large and the position of the mass minimum moves out to ever larger values of  $x$  as  $y$  increases. For example, if  $y = n = 1$  then  $m \gtrsim 400$  and lighter BH do not form. Such large mass values are far beyond the range accessible to the LHC if we assume  $M_* \sim 1$  TeV, *i.e.*, the interesting range roughly being  $1 \lesssim m \lesssim 10$  or so.<sup>¶</sup>

Since we are interested here in BH that can be created at colliders we will restrict our attention to smaller  $y$  values. In fact a short calculation shows that we need  $0.05 \lesssim y \lesssim 0.2$  in order to get into the LHC accessible mass region  $1 \lesssim m \lesssim 10$ . To demonstrate this we must find the minimum value of the BH mass,  $m_{min}$  as a function of  $y$  for various values of  $n$ . This can be

<sup>¶</sup>Note that we do not expect BH to form for masses much less than  $M_*$  so that it is reasonable to believe that  $m \gtrsim 1$ .

done in a two-step procedure: first we find where in  $x$  the mass minimum occurs for fixed values of  $y$ , *i.e.*, where  $\partial m/\partial x = 0$ . Calculating this derivative we see that the minimum can be obtained by solving the equation (using for convenience the variable  $q = x^2/4y^2$  introduced above):

$$F_n(q) - \frac{2q^{(n+3)/2}e^{-q}}{(n+1)\Gamma(\frac{n+3}{2})} = 0, \quad (17)$$

which has a single, non-zero root  $q_0(n)$ . For any  $y$  this tells us the value of the horizon radius where the minimum mass occurs,  $x_{min} = 2y\sqrt{q_0(n)}$ , which we can now use to obtain  $m_{min}$  employing the equations above. The result of this calculation is shown in Fig. 3. Here we see that for  $n$  in the range 1 to 7 the relevant values of  $y$  are rather narrow, not differing from  $y \simeq 0.1$  by more than about a factor of 2.

It is important to recall that for the ordinary commutative  $D$ -dimensional BH solution both  $m_{min}$  and  $x_{min}$  are algebraically zero. However, since we *believe* that  $m_{min} \gtrsim 1$  is required to produce a BH, stronger conditions are usually imposed. In our case the results shown in Fig. 3 represent the *algebraic* lower bound on  $m$  which certainly  $\rightarrow 0$  as  $\theta \rightarrow 0$ . Physically, we might crudely imagine that  $m_{min} \simeq \text{Max}(1, m_{min}^a)$  where  $m_{min}^a$  is the result shown in Fig. 3. We note that having a finite  $m_{min}$  implies a BH production threshold while a finite  $x_{min}$  implies a minimum BH production cross section,  $\sigma_{BH} \simeq \pi x_{min}^2/M_*^2$ , at colliders such as the LHC as is shown in Fig. 4. Here we see that far above threshold the BH production cross section scales like  $\sim m^{2/(n+1)}$  as would be expected in the commutative theory. However, for lighter BH this cross section falls significantly below this simple scaling rule and becomes quite small in the neighborhood of  $m_{min}$ , almost but not quite vanishing.

We can now focus on this region of small  $y$ ; for simplicity in what follows we will generally concentrate our results on the case  $y = 0.1$ . Fig. 5 shows  $m(x)$  for  $y = 0.1 - 0.2$  for  $n$  in the range 0 to 7. Note that *generally* larger  $n$  leads to smaller horizon radii for fixed  $y$  and already at  $y = 0.2$  we see explicitly that BH are too massive to be produced at the LHC as expected from the above

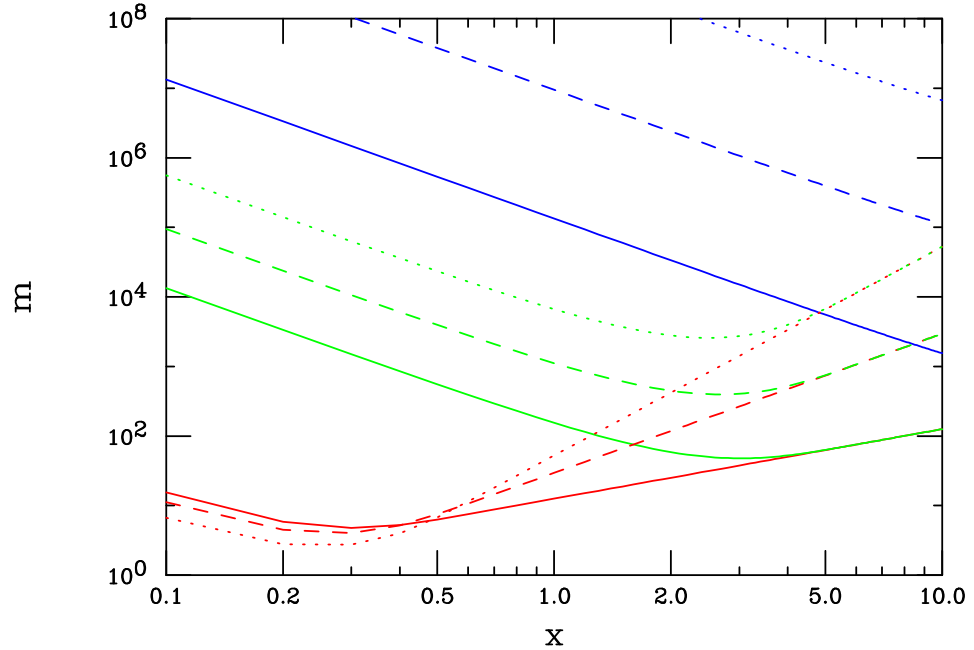


Figure 2: BH mass as a function of the horizon size for  $n = 0$ (solid),  $n = 1$ (dashed) and  $n = 2$ (dotted). The upper(middle, lower) set of curves correspond to  $y = 10(1, 0.1)$ .

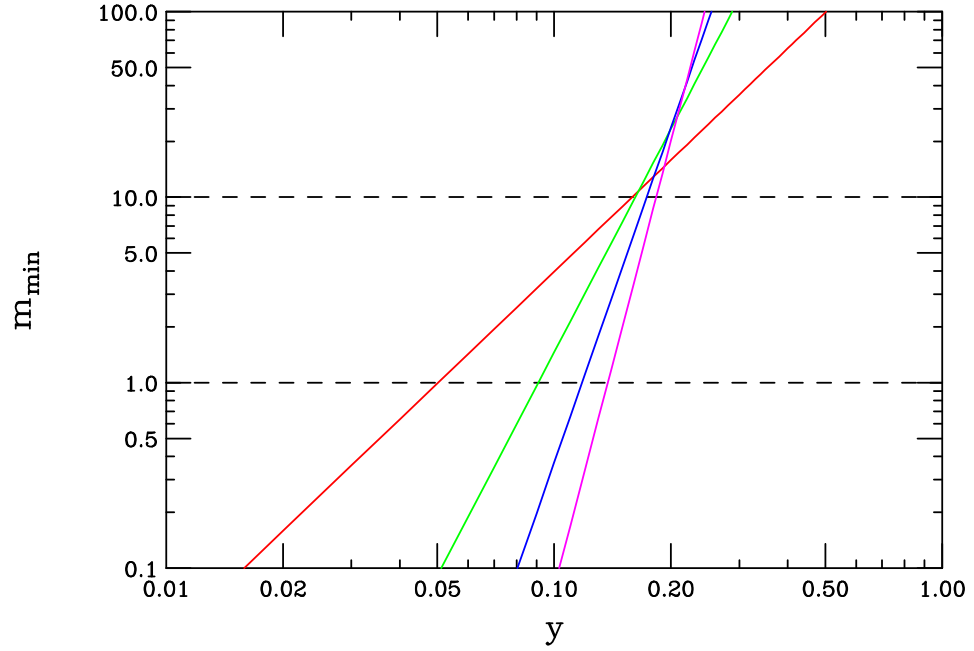


Figure 3: Minimum BH mass as a function of  $y$  showing the (very) approximate mass range accessible to the LHC between the dashed lines. On the left-hand side from top to bottom the curves correspond to  $n = 1, 3, 5$  and  $7$ , respectively. The allowed parameter range is above and to left of each curve.

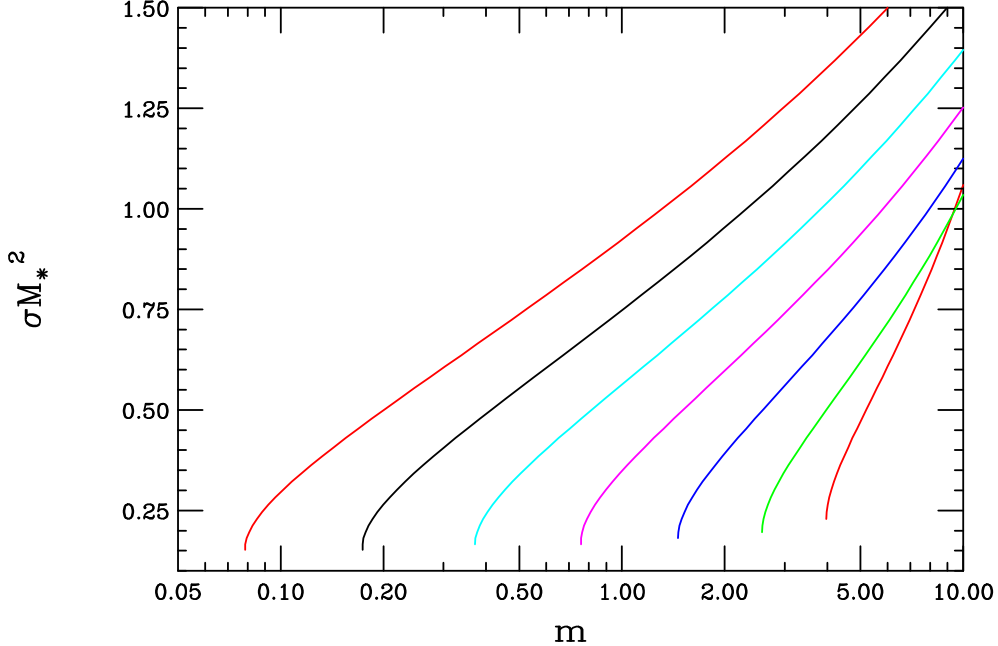


Figure 4: NC BH production subprocess cross section as a function of  $m$  for  $y = 0.1$ . From right to left at the bottom of the figure the curves correspond to  $n=1$  to  $7$ .

analysis if  $M_* \sim 1$  TeV. One also sees that at  $x \sim 1$  the asymptotic behavior,  $m \sim x^{n+1}$ , has already begun to set in for all  $n$ .

As an example of the insensitivity of these results to our assumed Gaussian parameterization of the smearing due to NC effects, let us briefly consider the modified Lorentzian form mentioned above. Setting  $y' = M_*\sqrt{\theta'} = 0.1$  (which is not necessarily the same as  $y = 0.1$ ), we again evaluate  $m$  as a function of  $x$ . The result of this calculation is shown in Fig. 6 which we should compare with the top panel of Fig. 5 that yields essentially the same result in the asymptotic large  $x \gtrsim 0.5$  (as it should since this is the commutative limit). In both cases a minimum mass occurs at relatively small  $x$  with somewhat similar values of  $m$ .  $m_{min}$  decreases in both cases as  $n$  is increased and the corresponding value of  $x_{min}$  also decreases as  $n$  is increased. The  $m_{min}$  values are seen to be quite comparable in the two cases. The greatest difference in the two results is seen to occur in the region of  $x$  below  $x_{min}$  where there is the most sensitivity to NC effects and the detailed shape of the assumed BH mass distribution. This is just what we would have expected; in the region

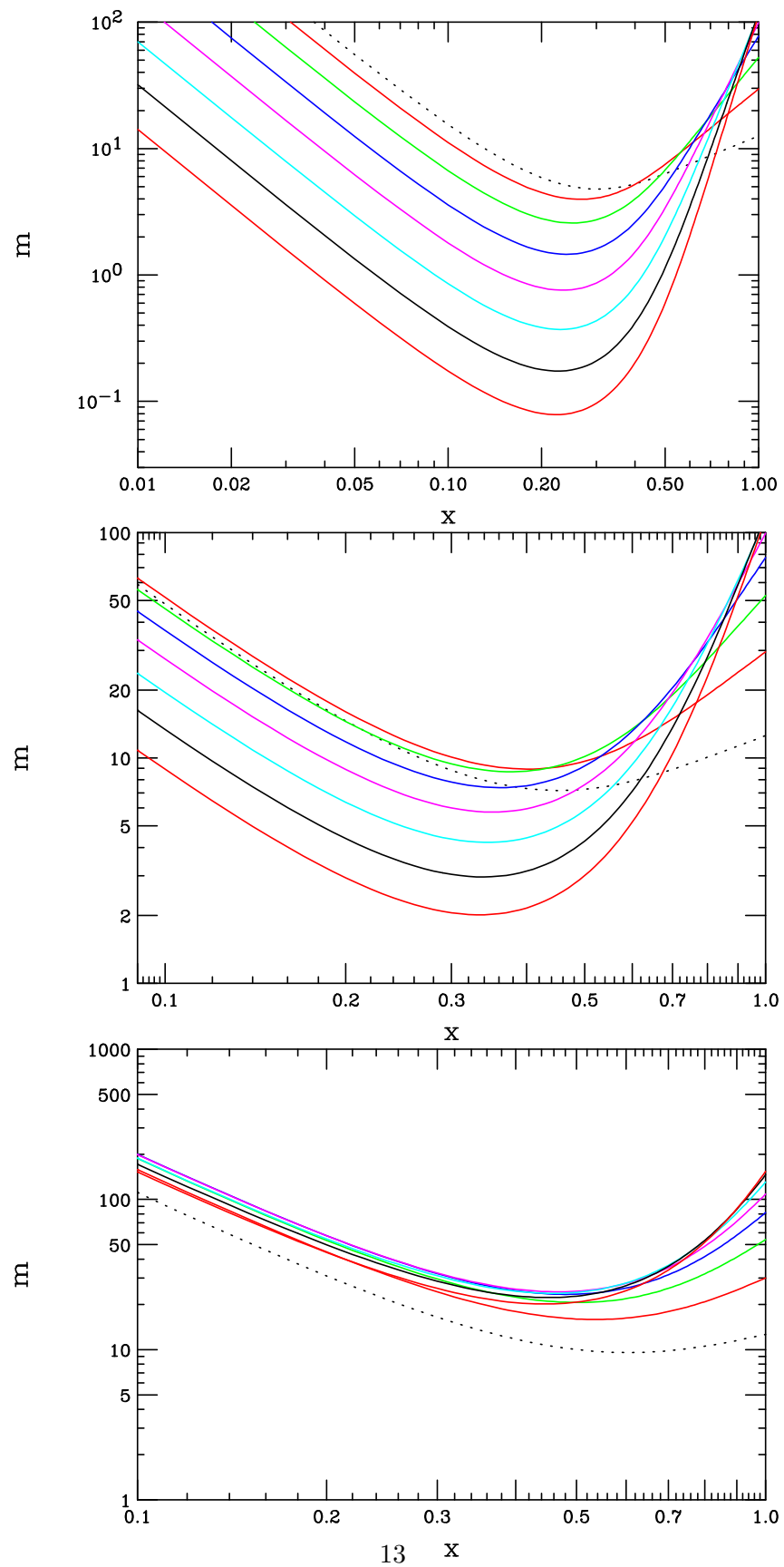


Figure 5: Same as in Fig. 2 but now for  $y = 0.10$ (top),  $0.15$ (middle) and  $0.20$ (bottom) with the dotted curve being for  $n = 0$ . From top to bottom on the left-hand side of the figure the solid curves are for  $n=1$  to  $7$ .

where NC effects just begin to be felt the detailed nature of the peaked mass distribution is not actually being probed. What is really being probed in this parameter range is the fact that there is a peaked mass distribution instead of a  $\delta$ -function source, *i.e.*, the BH has a form factor due its finite size, and not the details of its shape. Only at smaller values of the radii (relative to the values of  $y$  or  $y'$ ) do the differences in the details of the mass distribution become important. In fact, we can if we wish tune our chosen value of  $y'$  to make these two sets of curves even more alike. Since the majority of the effects we will discuss are sensitive only to physics with  $x \geq x_{min}$ , this short analysis shows that the general features of the results that we obtain below are not particularly sensitive to how the NC smearing of the mass distribution is performed.

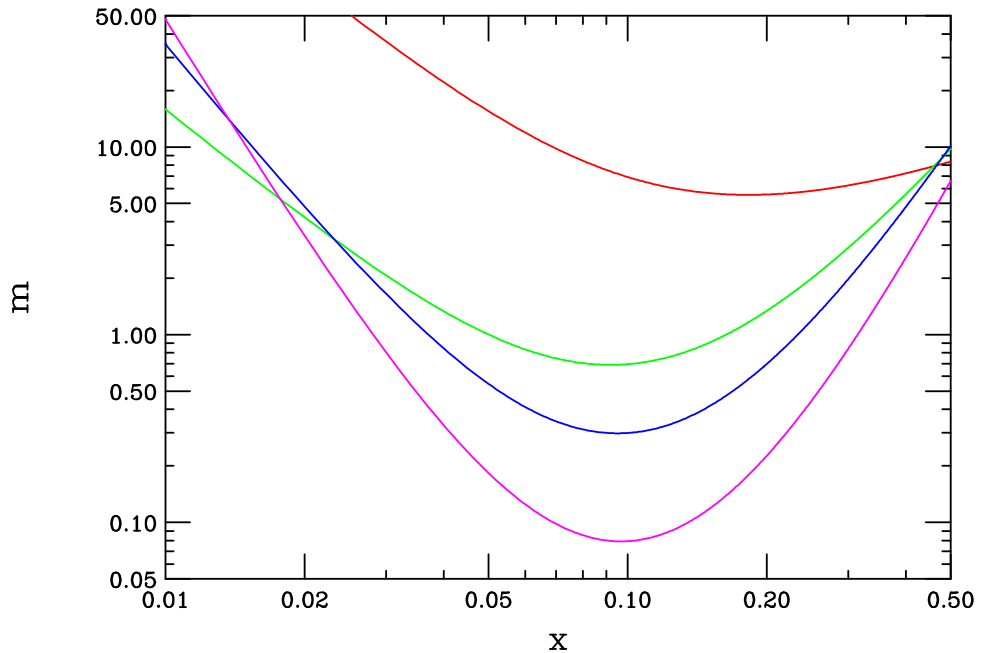


Figure 6: BH mass as a function of the horizon size  $x$  for  $y' = 0.1$  using Lorentzian smearing. From top to bottom in the middle of the figure the curves correspond to  $n = 0, 2, 4$  and  $6$ , respectively.

In order to understand the possibility of the formation of two (or no) horizons, we follow NSS and consider the metric tensor component  $g_{00}$  as a function of the dimensionless radius co-ordinate  $M_*r$  as shown in Fig. 7. Here we will assume that  $m = 5$ , a typical value which is kinematically accessible at LHC, for demonstration purposes. Recall that horizons occur when  $g_{00} = 0$ . With  $y = 0.1$  all of the curves pass through  $g_{00} = 0$  twice corresponding to two horizons, one on either

side of  $x_{min}$ . This explains why  $x(m)$  is double valued in Fig. 5, *i.e.*, the two solutions correspond to the two radii where  $g_{00}$  vanishes. For  $n = 0$ , the case studied by NSS, these two horizons are rather close in radius but this separation grows significantly as  $n$  increases. When  $y = 0.15$ , we see that for  $n = 0 - 4$  no horizon form as  $g_{00} \gtrsim 0.13$ . This corresponds to the result observed in Fig. 5 for  $y = 0.15$  where we see that for this range of  $n$  the value  $m = 5$  is not allowed. However, for  $n \geq 5$ , we again obtain two horizons; clearly a tuning of parameters will allow the two horizons to converge to the case of a single degenerate horizon at  $x_{min}$  as found by NSS. For both values of  $y$  we note that as  $M_*r \rightarrow 0$  the metric is no longer singular as in the pure Schwarzschild case as was noted by NSS in 4-d (as we are inside a well-behaved mass distribution), independently of the existence of any horizons. This is further confirmed by constructing the Ricci curvature invariant,  $R$ , as can be easily done from the Einstein equations above; in fact, we find that as  $x \rightarrow 0$ ,  $R \sim y^{-(n+3)}$ . Furthermore, and more explicitly, apart from an overall numerical factor,  $R \sim my^{-(n+3)}[n + 4 - \frac{(M_*r)^2}{2y^2}]e^{-(M_*r)^2/4y^2}$  so that  $R$  is seen to vanish as  $M_*r \rightarrow \infty$  as expected and undergoes a change of sign in the region, *e.g.*,  $M_*r \sim 0.2 - 0.5$  for  $y = 0.1$  independently of  $m$  and only weakly dependent on the value of  $n$ . As we will now see only the ‘outer’ horizon, *i.e.*, the one with  $x \geq x_{min}$  is actually relevant to us.

Our next step is to determine the thermodynamic behavior of these NC BH; to do this we first must calculate the Hawking temperature of the BH. This can be done in the usual manner by remembering that

$$T_H = \frac{1}{4\pi} \frac{de^\nu}{dr} \Big|_{r=x/M_*}, \quad (18)$$

*i.e.*, the temperature is essentially the  $r$  (radial) co-ordinate derivative of the metric evaluated at the horizon radius. Defining for convenience the dimensionless temperature,  $T = T_H/M_*$ , we obtain from the above form of the metric

$$T = \frac{n+1}{4\pi x} \left[ 1 - \frac{2q^{(n+3)/2}e^{-q}}{F_n(q)(n+1)\Gamma(\frac{n+3}{2})} \right]. \quad (19)$$

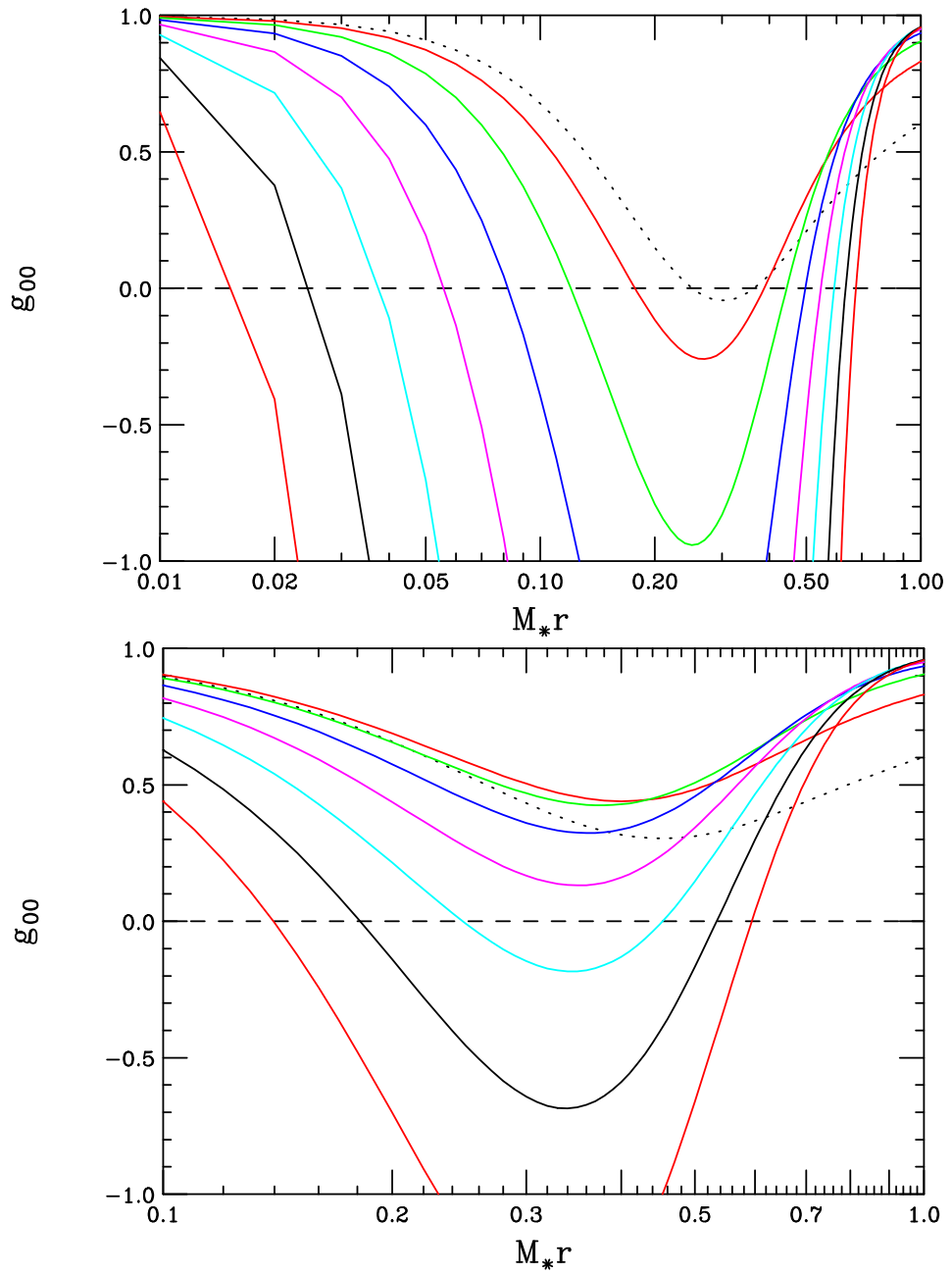


Figure 7:  $g_{00}$  as a function of  $M_*r$  assuming  $m = 5$  for either  $y = 0.10$ (top) or  $0.15$ (bottom). The dotted curve corresponds to  $n = 0$  while from top to bottom on the left-hand side of the figure the solid curves are for  $n=1$  to  $7$ . The dashed line corresponds to  $g_{00} = 0$ .

Note that as expected  $T$  returns to the usual commutative result in the  $q \rightarrow \infty$  limit, *i.e.*, the quantity in the large square bracket above  $\rightarrow 1$  in this limit. It is instructive to compare the temperature we obtain in both the NC and commutative cases for various values of the parameters; the ratio of these quantities is shown in Fig. 8. This ratio is seen to be near unity for large  $z$  as one would expect but it decreases rapidly as  $z$  approaches the  $\sim 2$ - $3$  range from above. The temperature is also seen to vanish at the same  $z$  value where the BH mass is minimized. For smaller  $z$ ,  $T$  becomes negative (which is where the second horizon occurs) and thus we enter a region that might usually be considered unphysical. If we had instead chosen the Lorentzian smearing these results would be quite similar qualitatively.

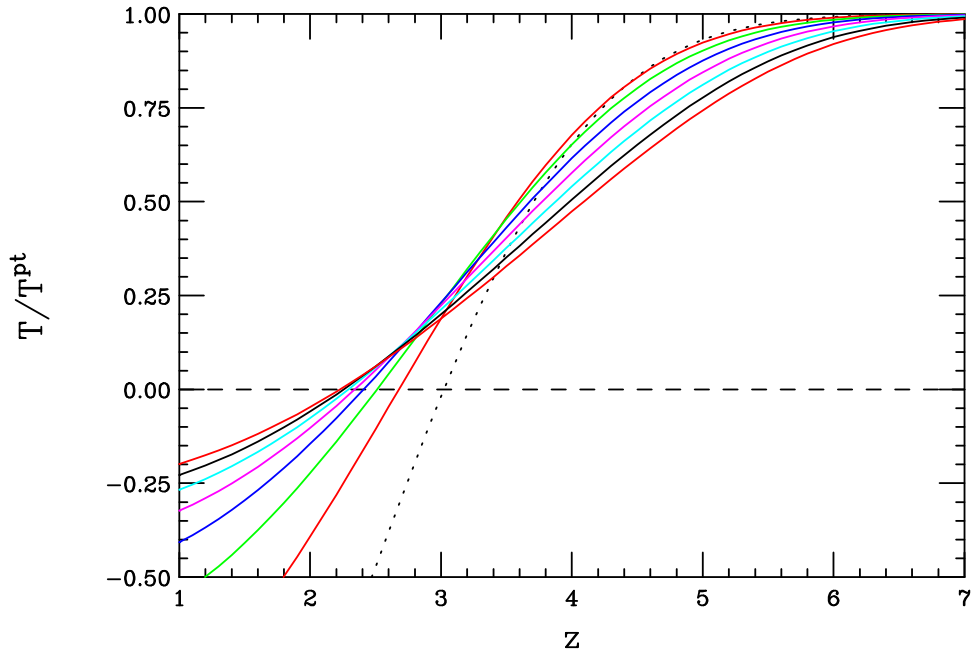


Figure 8: The ratio of the BH NC temperature to that obtained in the commutative limit where there is only a point matter source. The dotted curve corresponds to  $n = 0$  whereas, from bottom to top on the left-hand side of the figure, the solid lines correspond to  $n=1$  to  $7$ .

Fig. 9 shows the actual NC temperature as a function of  $x$  for  $y = 0.1$  and different  $n$  values. Here we see that  $T$  is quite close to its commutative value for  $x$  near unity, goes through a maximum as  $x$  decreases and then falls to zero at the BH mass minimum point. From these results and Fig. 5 above we can now trace the history of the entire semiclassical BH evaporation

process. <sup>||</sup> Consider a BH formed in a suitable parameter space region with moderately large values of  $m \sim 8 - 10$  (and, hence, with large  $x$ ). For such BH their Schwarzschild radii are too large to feel the effects of the NC scale in the formation process since  $x \gg y$ . As in the usual commuting picture, when the BH emits Hawking radiation it loses mass and gets hotter and thus radiates even more quickly. As the BH shrinks it begins to feel the NC effects and the temperature reaches a maximum in the mass region  $m \simeq 1 - 7$ , the specific number depending on the value of  $n$ . As the BH continues to lose mass its temperature now *decreases* so that it radiates ever more slowly. Finally, as  $m$  approaches  $m_{min}$  the semiclassical radiation emission processes ceases since  $T \rightarrow 0$  has been reached leaving a classically stable remnant. Though sounding somewhat unusual such a possibility has been discussed in the literature for a number of alternative BH scenarios which go beyond the basic picture presented by General Relativity based on just the EH action[10, 12]. <sup>\*\*</sup>

Whether quantum effects destabilize such a relic is not known.

It is easy to convince oneself that a classically stable remnant is the natural outcome of this scenario. In the usual treatment of BH decays, the mass loss rate (assuming a perfect radiator) is given by

$$\frac{dm}{dt} = -\Xi_d x^{d+2} T^{d+4}, \quad (20)$$

with  $\Xi_d$  being a positive numerical constant. For decays dominantly to bulk(brane) fields we have  $d = n(0)$ . In either case, clearly the lifetime of the BH is then given by

$$t_{BH} = -\Xi_d^{-1} \int_{m_{initial}}^{m_{min}} \frac{dm}{x^{d+2}(m) T^{d+4}(m)}, \quad (21)$$

with  $m_{initial}$  being the original BH mass. We recall from above that while  $x(m)$  is double valued it is well-behaved and never vanishes. However, on the otherhand, we also know that  $T(m) \rightarrow 0$  as  $m \rightarrow m_{min}$ . Thus for all  $n$  (and any  $d$ ),  $t_{BH}$  will be driven to infinity due to the presence of a

---

<sup>||</sup>Before beginning this discussion we must recall the usual argument discussed above that if  $m_{min}$  lies below  $\sim 1$  then no BH will form; we will ignore this prejudice in the following discussion treating  $m_{min}$  as the true minimum BH formation mass as derived from the theory itself.

<sup>\*\*</sup>These include models with higher curvature invariants in the action as well as those where a minimum length scale exists or where the Newton constant is taken to be a running parameter.

singular denominator in the integrand implying a stable relic. (Of course, an initial very massive BH will radiate down to a mass very close to  $m_{min}$  quite quickly.) This must happen in any model that predicts  $T \rightarrow 0$  at finite  $x$  due to a corresponding singularity. For the commuting case, since  $T \sim 1/x$ , the integrand is never singular so that the BH lifetime remains finite.

The lower panel in Fig. 9 summarizes this discussion where we see that as  $m$  decreases from a large value the temperature increases, reaches a maximum value and then falls to zero at  $m_{min}$  leaving a classically stable remnant.

This unusual temperature behavior in the NC case can also be studied more fully by examining the BH heat capacity/specific heat,  $C$ . In the commutative case,  $C$  is always finite (away from  $x = 0$ ) and negative since the BH gets hotter as it loses mass. Let we define

$$C = \frac{\partial m}{\partial T} = \frac{\partial m}{\partial x} \left( \frac{\partial T}{\partial x} \right)^{-1}, \quad (22)$$

which we can explicitly write as

$$C = -4\pi c_n x^{n+2} F_n(q)^{-1} \left[ \frac{1 - \frac{2H_n(q)}{(n+1)}}{1 - \frac{2H_n(q)}{(n+1)} + \frac{4qH_n(q)}{(n+1)} \left( \frac{(n+3)}{2q} - \frac{H_n(q)}{q} - 1 \right)} \right], \quad (23)$$

where for convenience we have defined the set of auxiliary functions

$$H_n(q) = \frac{q^{(n+3)/2} e^{-q}}{F_n(q) \Gamma(\frac{(n+3)}{2})}. \quad (24)$$

Using this expression, Fig. 10 shows the results for the NC BH heat capacity as a function of both  $x$  and  $m$  for our standard choice of  $y = 0.1$ . We first see that  $C$  remains negative at large  $x$  and asymptotes to its commutative value,  $C = -4\pi c_n x^{n+2}$ , as it should. Further we note that at  $x = x_{min}$  (or at  $m = m_{min}$ ) we find that  $C \rightarrow 0$  as was expected. BH with mass  $m_{min}$  are no longer capable of mass loss since they have zero temperature. Between these two regimes the

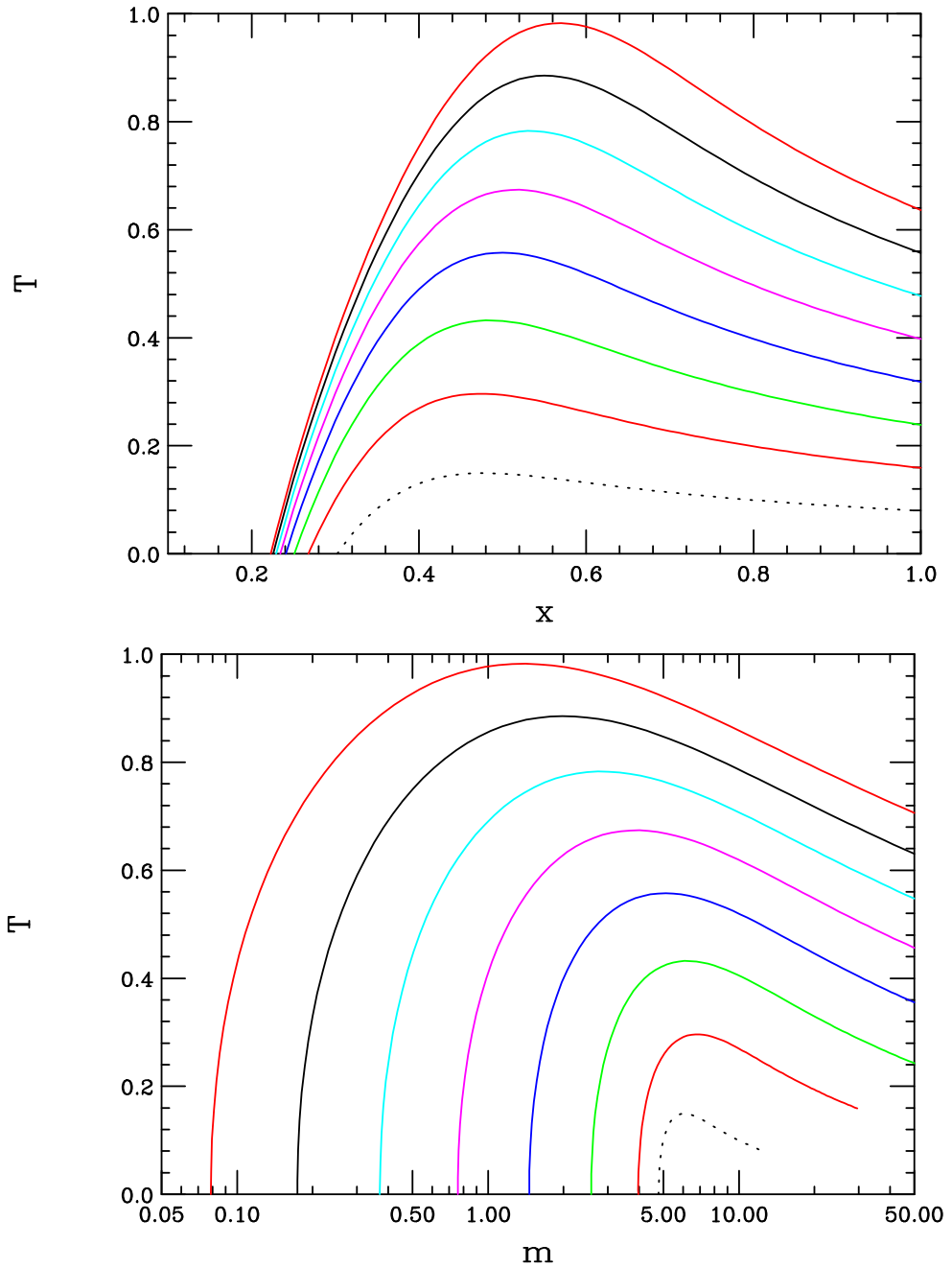


Figure 9: The NC BH temperature as a function of  $x$ (top panel) and  $m$ (lower panel) for fixed  $y = 0.1$ . The dotted curve corresponds to case of  $n = 0$  whereas, from bottom to top on the right-hand side of the figure, the solid lines correspond to  $n=1$  to  $7$ .

behavior of  $C$  is quite interesting. Consider  $C$  as a function of large and decreasing  $x$ .  $C$  at first decreases in magnitude as it does in the commutative case. However as we know from above, for some  $n$ -dependent  $x$  value,  $T$  reaches a maximum and then decreases. This implies that the magnitude of  $C$  then increases and becomes singular for this particular  $x$  value. For lower  $x$  the sign of  $C$  changes as now  $\frac{\partial T}{\partial x} > 0$  and then approaches zero at  $m_{min}$ . This is even more obvious when we consider  $C$  as a function of  $m$ . For large  $m$  the BH radiates as in the commutative case as  $C$  decreases in magnitude as  $m$  is reduced. However, at some point the NC effects turn on and  $-C$  begins to increase, becoming singular where  $\frac{\partial T}{\partial m} = 0$ , the location of temperature the maximum. For smaller masses, as the BH radiates and gets lighter the temperature decreases so that we are now in a region of positive heat capacity. As  $m$  decreases further to  $m_{min}$ ,  $C$  becomes zero for the remnant.

Our next step in examining the thermodynamics of NC BH is to consider the value of the entropy which is defined via

$$S = \int dx T^{-1} \frac{\partial m}{\partial x} = 4\pi c_n \int_{x_{min}}^x dv \frac{v^{n+1}}{F_n(v^2/4y^2)}, \quad (25)$$

where here we have made the natural choice that the entropy vanish at  $x_{min}$  where the BH mass  $m$  is minimized for fixed values of  $y$  and  $n$ . In the commutative limit where  $\theta, y \rightarrow 0$  then  $x_{min} \rightarrow 0$  and we recover the usual lower limit of integration. Fig. 11 shows the values of the entropy for various  $n$  as a functions of  $x$  or  $m$  for our canonical choice of  $y = 0.1$ . We again observe that the commutative power law behavior,  $S = 4\pi c_n \frac{x^{n+2}}{(n+2)}$ , is recovered in the large  $x \gtrsim 1$  limit as expected. It is more interesting to consider  $S$  as a function of  $m$ ; as we see from the Figure, while the entropy scales as  $\sim m^{(n+2)/(n+1)}$  for large  $m$  it rapidly falls below this scaling law to zero as  $m$  approaches  $m_{min}$  from above.

Finally, we also examine the free energy of the NC BH which is simply given by combining

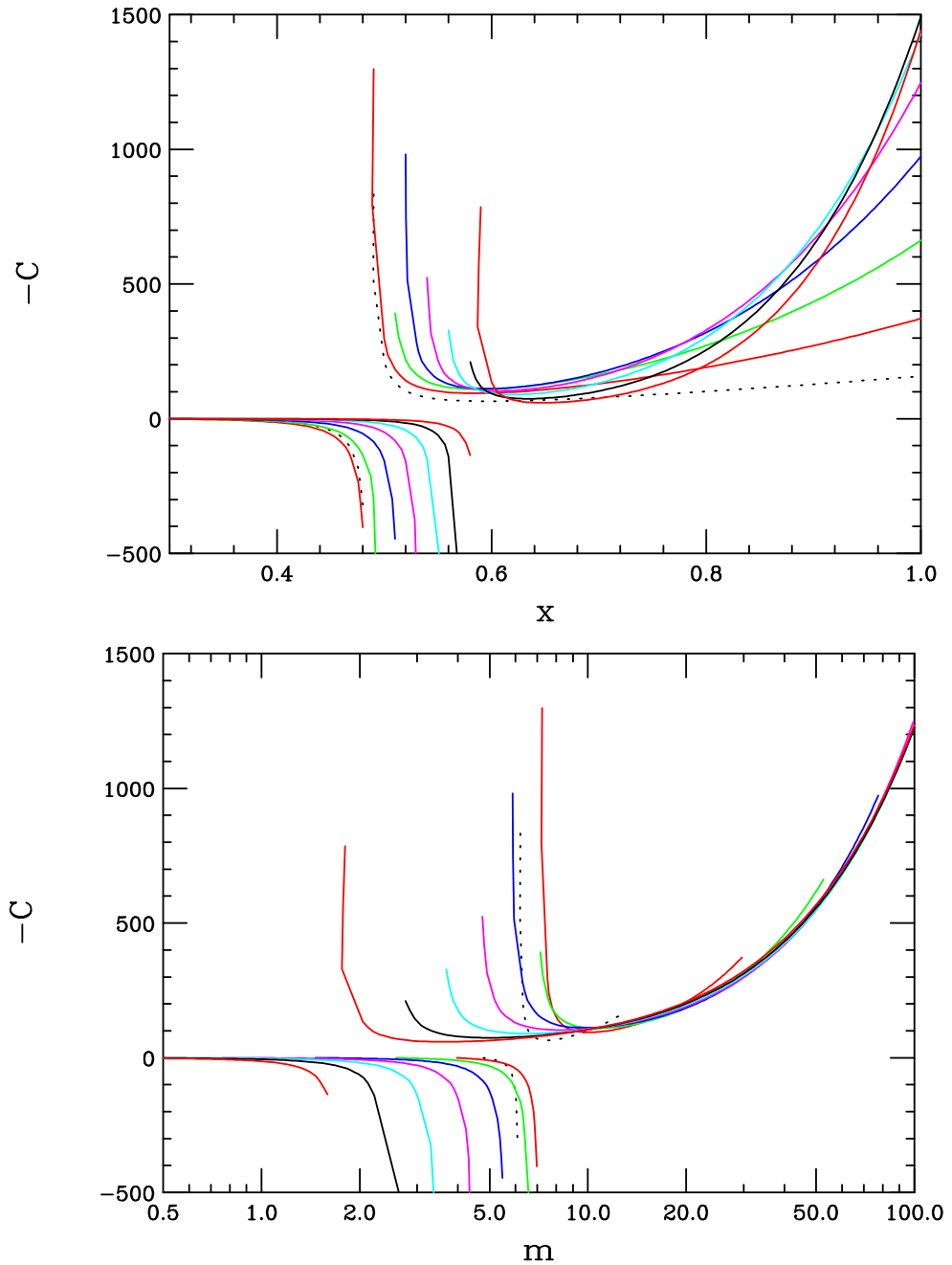


Figure 10: Negative of the NC BH heat capacity/specific heat as a function of  $x$ (top panel) and  $m$ (bottom panel) for fixed  $y = 0.1$ . The dotted curve corresponds to case of  $n = 0$  whereas, from bottom to top in the middle of the figure, the solid lines correspond to  $n=1$  to  $7$ . In the bottom panel, the parameter region with negative temperatures has been removed.

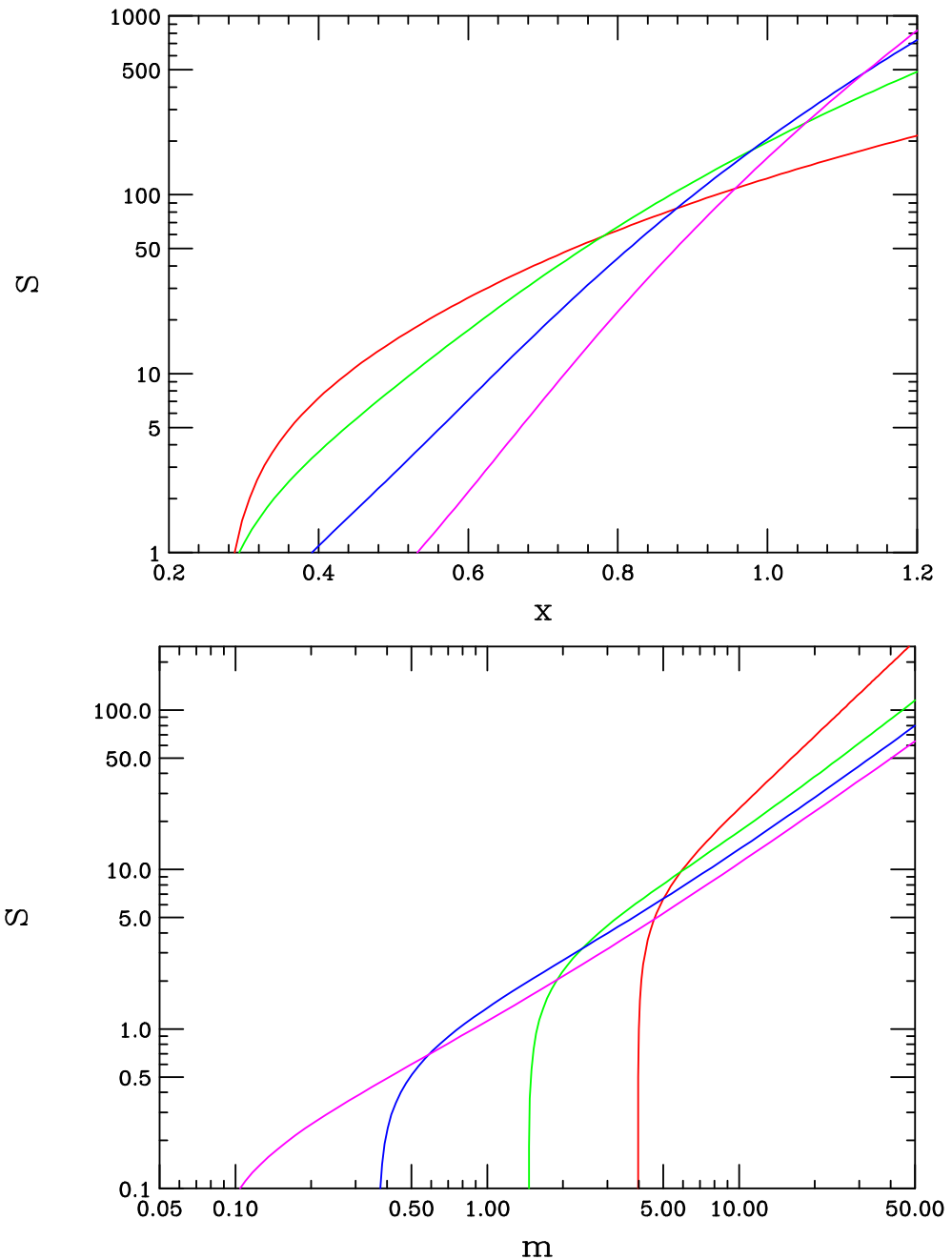


Figure 11: The NC BH entropy as a function of  $x$  (top panel) and  $m$  (bottom panel) for fixed  $y = 0.1$ . From left to right (right to left) at the bottom of the top (bottom) panel the the curves are for  $n = 1, 3, 5$  and  $7$ , respectively.

the above thermodynamic quantities:

$$F = m - TS. \quad (26)$$

As seen in Fig. 12, it too returns to its commutative value,  $F = m/(n+2)$ , in the limit of large  $x \gtrsim 1$  or large  $m$ . However, for  $x = x_{min}$  it is clear that  $F = m$  for all values of  $y$  and  $n$  since both  $T$  and (by definition)  $S$  vanish at this point. Immediately above  $x = x_{min}$  (or  $m_{min}$ ),  $F$  decreases slightly, until it matches onto the asymptotic  $\sim x^{n+1}$  behavior. For some parameter values  $F$  can even become negative in this intermediate mass regime. Generally we see the unusual behavior that  $m = m_{min}$  is *not* the location of a minimum in  $F$  as either a function of  $x$  or  $m$ . This minimum lies near the values of  $x$  and  $m$  where  $T$  is maximized.

### 3 Discussion and Conclusions

Space-time noncommutativity and extra dimensions are both well-motivated ideas within the string theory context and it is natural for them to make their appearance felt as one approaches the fundamental scale. In more than four dimensions it is possible for this scale to be not far from  $\sim$  TeV and thereby address the gauge hierarchy problem. If this mass parameter is indeed this low it is likely that black holes will be produced at the LHC in sufficient quantities that their properties will be well measured. The occurrence of NC also at a similar scale could lead to significant modifications in the anticipated properties of these BH. Since a complete NC theory of gravity does not yet exist it becomes necessary to model the NC effects within the commutative General Relativity framework.

Nicolini, Smailagic and Spallucci presented a physically motivated model of this kind in 4-d, where the essential aspects were the Gaussian smearing of matter distributions on the NC scale and the continued applicability of the EH action. They then went on to examine NC effects on BH physics. In this paper we extended this NC BH analysis in several ways: (i) we generalized the NSS study to the case of extra dimensions with a fundamental scale in the TeV range so that

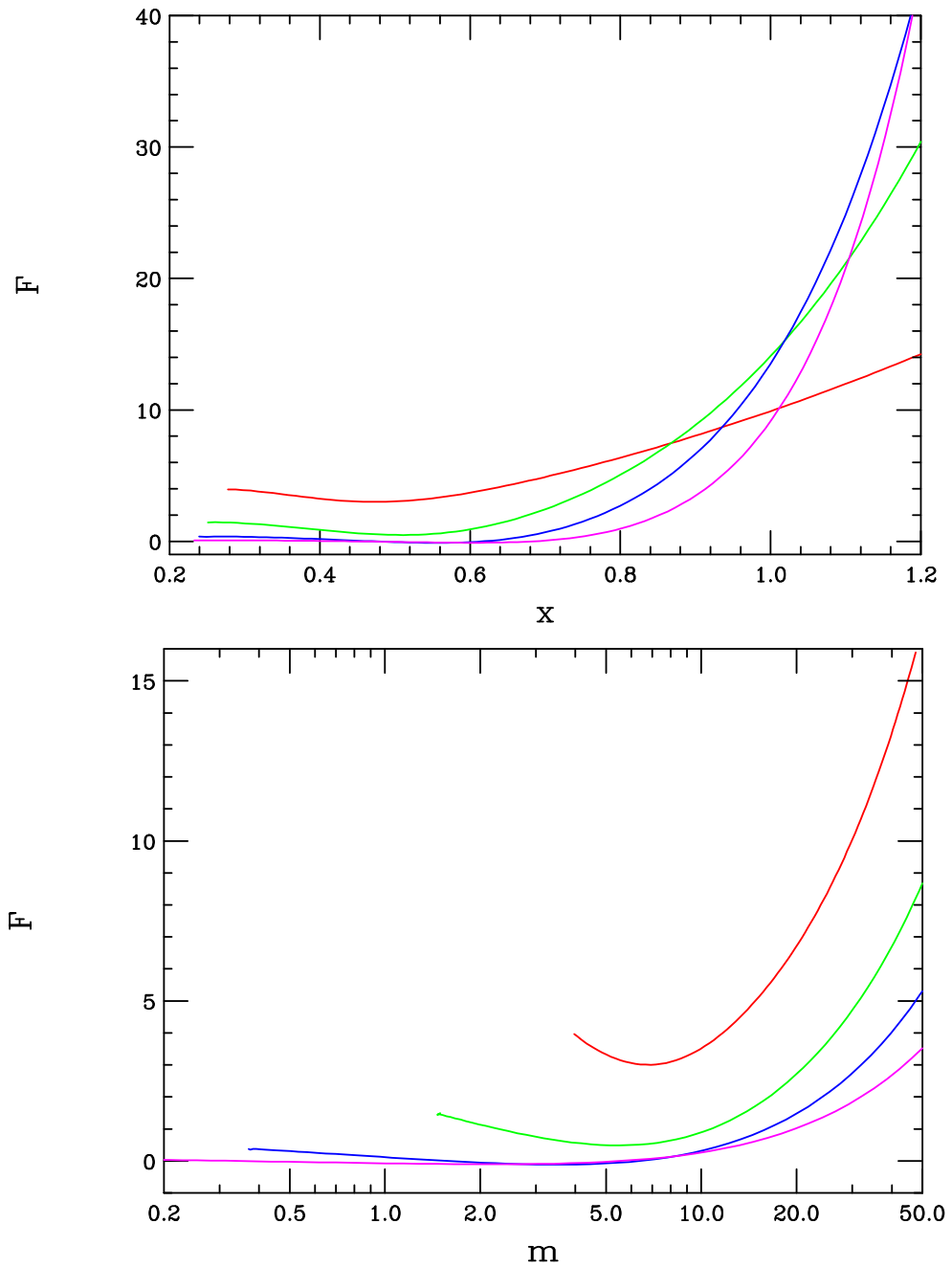


Figure 12: The NC BH free energy as a function of  $x$  (top panel) and  $m$  (bottom panel) for  $y = 0.1$ . From top to bottom on the left-hand side the curves correspond to  $n = 1, 3, 5$  and  $7$ , respectively

the associated BH can be produced with large cross sections and studied in detail at the LHC. While much of the BH behavior observed in extra dimensions was similar to that obtained in 4-d, some significant modifications to the previously obtained 4-d results were observed. However, there appears to be an overall dominance of NC effects over those that arise due to the existence of the extra dimensions. *(ii)* We demonstrated that the essential physics induced by NC smearing is not particularly sensitive to the assumed nature of the smearing function. In particular we explicitly showed that Gaussian and Lorentzian smearing lead to essentially the same behavior for the expected modifications of the BH mass-radius relationship due to NC effects. *(iii)* We extended the NSS analysis to include several other thermodynamic quantities which are of interest in the study of NC BH such as their entropy, heat capacity and free energy.

Perhaps the most important qualitative influence of NC on BH physics was already observed in 4-d by NSS, *i.e.*, the existence of a classically stable remnant whose mass and radius are completely fixed by the NC scale and the number of dimensions. Within the framework of extra dimensions, if the fundamental scale is not too large then BH and their remnants will be copiously produced at the LHC and studied in detail. The observation of NC effects in the properties of these BH can open a new window on the fundamental theory of gravity and space-time.

## Acknowledgments

The author would like to thank J.L. Hewett and B. Lillie for discussions related to this work.

## References

- [1] For very early work on NC, see H. S. Snyder, Phys. Rev. **72**, 68 (1947).
- [2] This is a huge subject; some basic references are A. Connes, *Non-commutative Geometry*, (Academic Press, New York, 1994); M. R. Douglas and N. A. Nekrasov, Rev. Mod. Phys. **73**, 977 (2001) [arXiv:hep-th/0106048]; N. Seiberg and E. Witten, JHEP **9909**, 032

(1999) [arXiv:hep-th/9908142]; M. R. Douglas and C. M. Hull, JHEP **9802**, 008 (1998) [arXiv:hep-th/9711165]; A. Connes, M. R. Douglas and A. S. Schwarz, JHEP **9802**, 003 (1998) [arXiv:hep-th/9711162]; N. Seiberg, L. Susskind and N. Toumbas, JHEP **0006**, 021 (2000) [arXiv:hep-th/0005040] and JHEP **0006**, 044 (2000) [arXiv:hep-th/0005015]; R. Gopakumar, J. M. Maldacena, S. Minwalla and A. Strominger, JHEP **0006**, 036 (2000) [arXiv:hep-th/0005048]; M. M. Sheikh-Jabbari, Phys. Lett. B **455**, 129 (1999) [arXiv:hep-th/9901080]; D. J. Gross, A. Hashimoto and N. Itzhaki, Adv. Theor. Math. Phys. **4**, 893 (2000) [arXiv:hep-th/0008075]; D. Bigatti and L. Susskind, Phys. Rev. D **62**, 066004 (2000) [arXiv:hep-th/9908056]; T. Pengpan and X. Xiong, Phys. Rev. D **63**, 085012 (2001) [arXiv:hep-th/0009070]; J. L. F. Barbon and E. Rabinovici, Phys. Lett. B **486**, 202 (2000) [arXiv:hep-th/0005073]; J. Gomis, M. Kleban, T. Mehen, M. Rangamani and S. H. Shenker, JHEP **0008**, 011 (2000) [arXiv:hep-th/0003215]; J. Gomis, T. Mehen and M. B. Wise, JHEP **0008**, 029 (2000) [arXiv:hep-th/0006160]; E. T. Akhmedov, P. DeBoer and G. W. Semenoff, Phys. Rev. D **64**, 065005 (2001) [arXiv:hep-th/0010003]; J. Gomis, K. Kamimura and T. Matheos, JHEP **0103**, 010 (2001) [arXiv:hep-th/0009158]. A. Rajaraman and M. Rozali, JHEP **0004**, 033 (2000) [arXiv:hep-th/0003227]; J. W. Moffat, Phys. Lett. B **491**, 345 (2000) [arXiv:hep-th/0007181]; F. Lizzi, G. Mangano and G. Miele, Mod. Phys. Lett. A **16**, 1 (2001) [arXiv:hep-th/0009180].

- [3] X. Calmet, B. Jurco, P. Schupp, J. Wess and M. Wohlgenannt, Eur. Phys. J. C **23**, 363 (2002) [arXiv:hep-ph/0111115]; B. Jurco, L. Moller, S. Schraml, P. Schupp and J. Wess, Eur. Phys. J. C **21**, 383 (2001) [arXiv:hep-th/0104153]; J. Madore, S. Schraml, P. Schupp and J. Wess, Eur. Phys. J. C **16**, 161 (2000) [arXiv:hep-th/0001203]; M. Hayakawa, Phys. Lett. B **478**, 394 (2000) [arXiv:hep-th/9912094]; K. Matsubara, Phys. Lett. B **482**, 417 (2000) [arXiv:hep-th/0003294]; M. Chaichian, P. Presnajder, M. M. Sheikh-Jabbari and A. Tureanu, Eur. Phys. J. C **29**, 413 (2003) [arXiv:hep-th/0107055] and Phys. Lett. B **526**, 132 (2002) [arXiv:hep-th/0107037];

S. Marculescu, arXiv:hep-th/0508018.

- [4] There has been a huge amount of work on this subject; see, for example, I. Hinchliffe, N. Kersting and Y. L. Ma, *Int. J. Mod. Phys. A* **19**, 179 (2004) [arXiv:hep-ph/0205040]; J. L. Hewett, F. J. Petriello and T. G. Rizzo, *Phys. Rev. D* **66**, 036001 (2002) [arXiv:hep-ph/0112003] and *Phys. Rev. D* **64**, 075012 (2001) [arXiv:hep-ph/0010354]; C. D. Carone and H. J. Kwee, arXiv:hep-ph/0603137; A. Alboteanu, T. Ohl and R. Ruckl, PoS **HEP2005**, 322 (2006) [arXiv:hep-ph/0511188]. B. Melic, K. Passek-Kumericki, J. Trampetic, P. Schupp and M. Wohlgenannt, *Eur. Phys. J. C* **42**, 499 (2005) [arXiv:hep-ph/0503064]. T. Ohl and J. Reuter, arXiv:hep-ph/0407337; X. Calmet, *Eur. Phys. J. C* **41**, 269 (2005) [arXiv:hep-ph/0401097]; G. Duplancic, P. Schupp and J. Trampetic, *Eur. Phys. J. C* **32**, 141 (2003) [arXiv:hep-ph/0309138]; J. M. Conroy, H. J. Kwee and V. Nazaryan, *Phys. Rev. D* **68**, 054004 (2003) [arXiv:hep-ph/0305225]; N. Mahajan, *Phys. Rev. D* **68**, 095001 (2003) [arXiv:hep-ph/0304235]; P. Schupp, J. Trampetic, J. Wess and G. Raffelt, *Eur. Phys. J. C* **36**, 405 (2004) [arXiv:hep-ph/0212292]; C. E. Carlson, C. D. Carone and N. Zobin, *Phys. Rev. D* **66**, 075001 (2002) [arXiv:hep-th/0206035]; E. O. Iltan, *Phys. Rev. D* **66**, 034011 (2002) [arXiv:hep-ph/0204332]; Z. Chang and Z. z. Xing, *Phys. Rev. D* **66**, 056009 (2002) [arXiv:hep-ph/0204255]; X. G. He, *Eur. Phys. J. C* **28**, 557 (2003) [arXiv:hep-ph/0202223]; W. Behr, N. G. Deshpande, G. Duplancic, P. Schupp, J. Trampetic and J. Wess, *Eur. Phys. J. C* **29**, 441 (2003) [arXiv:hep-ph/0202121]; N. G. Deshpande and X. G. He, *Phys. Lett. B* **533**, 116 (2002) [arXiv:hep-ph/0112320]; C. E. Carlson and C. D. Carone, *Phys. Rev. D* **65**, 075007 (2002) [arXiv:hep-ph/0112143].; S. Godfrey and M. A. Doncheski, *Phys. Rev. D* **65**, 015005 (2002) [arXiv:hep-ph/0108268]; H. Grosse and Y. Liao, *Phys. Rev. D* **64**, 115007 (2001) [arXiv:hep-ph/0105090] and *Phys. Lett. B* **520**, 63 (2001) [arXiv:hep-ph/0104260].
- [5] See, for example, X. Calmet and A. Kobakhidze, *Phys. Rev. D* **72**, 045010 (2005) [arXiv:hep-th/0506157] and arXiv:hep-th/0605275; A. H. Chamseddine, *Phys. Lett. B* **504**, 33

- (2001) [arXiv:hep-th/0009153]; P. Aschieri, C. Blohmann, M. Dimitrijevic, F. Meyer, P. Schupp and J. Wess, *Class. Quant. Grav.* **22**, 3511 (2005) [arXiv:hep-th/0504183]; P. Mukherjee and A. Saha, arXiv:hep-th/0605287; L. Alvarez-Gaume, F. Meyer and M. A. Vazquez-Mozo, arXiv:hep-th/0605113.
- [6] P. Nicolini, A. Smailagic and E. Spallucci, *Phys. Lett. B* **632**, 547 (2006) [arXiv:gr-qc/0510112].
- [7] N. Arkani-Hamed, S. Dimopoulos and G. R. Dvali, *Phys. Rev. D* **59**, 086004 (1999) [arXiv:hep-ph/9807344] and *Phys. Lett. B* **429**, 263 (1998) [arXiv:hep-ph/9803315]; I. Antoniadis, N. Arkani-Hamed, S. Dimopoulos and G. R. Dvali, *Phys. Lett. B* **436**, 257 (1998) [arXiv:hep-ph/9804398].
- [8] L. Randall and R. Sundrum, *Phys. Rev. Lett.* **83**, 3370 (1999) [arXiv:hep-ph/9905221].
- [9] G. F. Giudice, R. Rattazzi and J. D. Wells, *Nucl. Phys. B* **544**, 3 (1999) [arXiv:hep-ph/9811291]; T. Han, J. D. Lykken and R. J. Zhang, *Phys. Rev. D* **59**, 105006 (1999) [arXiv:hep-ph/9811350]; E. A. Mirabelli, M. Perelstein and M. E. Peskin, *Phys. Rev. Lett.* **82**, 2236 (1999) [arXiv:hep-ph/9811337]; J. L. Hewett, *Phys. Rev. Lett.* **82**, 4765 (1999) [arXiv:hep-ph/9811356]; For a review, see J. Hewett and M. Spiropulu, *Ann. Rev. Nucl. Part. Sci.* **52**, 397 (2002) [arXiv:hep-ph/0205106].
- [10] T. Banks and W. Fischler, hep-th/9906038; S. Dimopoulos and G. Landsberg, *Phys. Rev. Lett.* **87**, 161602 (2001) [arXiv:hep-ph/0106295]; S. B. Giddings and S. Thomas, *Phys. Rev. D* **65**, 056010 (2002) [arXiv:hep-ph/0106219]; For a recent review, see P. Kanti, arXiv:hep-ph/0402168. For details of the present notation and further original references, see T. G. Rizzo, *JHEP* **0506**, 079 (2005) [arXiv:hep-ph/0503163].
- [11] J. L. Hewett, B. Lillie and T. G. Rizzo, *Phys. Rev. Lett.* **95** (2005) 261603 [arXiv:hep-ph/0503178].

[12] A. Bonanno and M. Reuter, Phys. Rev. D **62**, 043008 (2000) [arXiv:hep-th/0002196]. See also B. F. L. Ward, arXiv:hep-ph/0605054; M. Cavaglia, S. Das and R. Maartens, Class. Quant. Grav. **20**, L205 (2003) [arXiv:hep-ph/0305223] and references therein. See also, S. Hossenfelder, Phys. Lett. B **598**, 92 (2004) [arXiv:hep-th/0404232]; M. Bojowald, R. Goswami, R. Maartens and P. Singh, gr-qc/0503041; T. G. Rizzo in Ref.[10]